SPANDIDOS PUBLICATIONS

Comparative metabolic profiling of paediatric ependymoma, medulloblastoma and pilocytic astrocytoma

S. CUELLAR-BAENA[1], J.M. MORALES[2], H. MARTINETTO[3], J. CALVAR[3], G. SEVLEVER[3], G. CASTELLANO[1], M. CERDA-NICOLAS[4], B. CELDA[5] and D. MONLEON[6]

[1]Instituto de Física 'Gleb Wataghin', Universidade Estadual de Campinas, UNICAMP, Brazil; [2]Unidad Central de Investigación en Medicina, Universitat de València, Spain; [3]Fundación para la Lucha de Enfermedades Neurológicas de la Infancia (FLENI), Argentina; [4]Departamento de Patología, Universitat de Valencia, Spain; [5]Departamento de Química Física, Universitat de València, Spain; [6]Fundación de Investigación del Hospital Clínico Universitario de Valencia/INCLIVA, Valencia, Spain

Received April 27, 2010; Accepted July 3, 2010

DOI: 10.3892/ijmm_00000546

Abstract. Brain tumours are the most common solid tumours in children and a major cause of childhood mortality. The most common paediatric brain tumours include ependymomas, cerebellar astrocytomas and medulloblastomas. These brain tumours are highly heterogeneous regarding their histology, prognosis and therapeutic response. Subtle biochemical changes can be detected in intact tissues by High-Resolution Proton Magnetic Angle Spinning Spectroscopy (HR-MAS) revealing the status of tumour microheterogeneity and metabolic alterations before they are morphologically detectable. In this study, we present metabolic profiles by HR-MAS of 20 intact tissue samples from paediatric brain tumours. Tumour types include ependymoma, medulloblastoma and pilocytic astrocytoma. The metabolic characterization of paediatric brain tumour tissue by HR-MAS spectroscopy provided differential patterns for these tumours. The metabolic composition of the tumour tissue was highly consistent with previous *in vivo* and *ex vivo* studies. Some resonances detected in this work and not previously observed by *in vivo* spectroscopy also show potential in determining tumour type and grade (fatty acids, phenylalanine, glutamate). Overall, this work suggests that the additional information obtained by NMR metabolic profiling applied to tissue from paediatric brain tumours may be useful for assessing tumour grade and determining optimum treatment strategies.

Correspondence to: Dr Daniel Monleón, Fundación de Investigación del Hospital Clínico Universitario de Valencia, Avda. Blasco Ibánez, 17, Valencia 46010, Spain

E-mail: daniel.monleon@uv.es

Key words: paediatric brain tumors, ependymoma, medulloblastoma, pilocytic astrocytoma, biochemical profiling, High-Resolution Proton Magnetic Angle Spinning Spectroscopy, metabolic profiling

Introduction

Brain tumours are the most common solid tumours in children and a major cause of childhood mortality. The most common paediatric brain tumours include cerebellar astrocytomas, medulloblastomas and ependymomas. These paediatric brain tumours are highly heterogeneous regarding histology, prognosis and therapeutic response (1-4). Medulloblastomas, the most frequent malignant CNS neoplasm in children, usually located in the mid-line, are characterized, such as other embryonic neuroepithelial tumours, by undifferentiated cells. They are classified as WHO grade IV, and are among the most aggressive types of tumours that affect children (4,5). Many medulloblastomas appear on MRI images as solid, contrast-enhancing masses dropping from the vermis into the ventricular cavity of the fourth ventricle (2). Their metabolic profiles have been characterized mostly by *in vivo* spectroscopy in 1.5 T clinical scanners (6-11). The predominant and most characteristic metabolic feature of medulloblastoma with respect to other types of tumours is higher levels of taurine. Ependymomas, on the other hand, constitute 5-7% of all CNS intracranial tumours and are predominantly present in the first two decades of life. The fourth ventricle is the most common location for ependymomas. Cellular and anaplastic ependymoma are WHO grades II and III, respectively (12). Despite *in vivo* MRS spectra from both cellular and anaplastic ependymomas exhibiting considerable heterogeneity, their metabolic common profile include lower relative levels of N-acetyl-aspartate (NAA) in comparison to other tumours (6-11). Prognosis, treatment strategy and survival rates in cases of medulloblastoma and ependymoma depend on many factors. Children with aggressive tumour pathologies are stratified for therapeutic purposes according to age and metastatic status, factors that also determine the neurological side effects after surgical resection (4). On the contrary, pilocytic astrocytomas are usually indolent tumours that have longer survival rates. Pylocytic astrocytomas in childhood are WHO grade I tumours with the cerebellum as the most common anatomic site of origin (13). MRI of pilocytic astro-

Table I. Patient demographics including tumour type, WHO grade, localization, number of cases, mean age of patients and gender distribution.

Diagnosis	WHO grade	Localization	N	Age	Gender
Pilocytic astrocytoma	I	Cerebellum, frontal, supracellar region	8	7.6±4.1	4 F/4 M
Ependymoma	II	Ventricular, cerebellum	3	5.0±3.5	1 F/2 M
Anaplastic ependymoma	III	Ventricular	2	3.0±0.0	1 F/1 M
Medulloblastoma	IV	Cerebellum, ventricular	7	7.0±4.4	4 F/3 M

N, number of cases; F, female; M, male.

cytomas shows the typical macroscopic appearance of a well-demarcated lesion with a solid nodule and a cystic component (2). Low levels of creatine, myo-inositol and taurine are the most relevant features of the *in vivo* MRS metabolic profile of pylocytic astrocytoma (6-11,14). Overall, *in vivo* MRS biomarkers may help in the non-invasive diagnosis of paediatric brain tumours (6-11,15). However, *in vivo* MRS of paediatric brain tumours still exhibits some limitations. First, the tumour size in paediatric patients is often smaller than the optimum voxel size, leading to contamination problems often results for magnetic field susceptibility artefacts. Second, magnetic field strength and, therefore spectral resolution, is limited in clinical environments. Global metabolic profiles by high resolution NMR, performed on tumour tissue obtained at surgery, may support diagnosis when the conventional approaches are not sufficient.

High-Resolution Proton Magnetic Angle Spinning Spectroscopy (^{1}H HR-MAS) is a powerful technique being broadly applied in metabolic profiling of intact tissues (16,17), cells and biofluids (18,19), which has also been successfully applied to the characterization of different types of cancers (20-22). Subtle biochemical changes detected in intact tissues (*ex vivo*) by ^{1}H HR-MAS reveal the status of tumour micro-heterogeneity, and provide information on tumour metabolic alterations before they are morphologically detectable. They also may correlate to histopathological features and diagnosis. Thus, the precise determination of biochemical and metabolic profiles in intact tissue promises to extend the possibilities of high resolution MR spectroscopy as a medical diagnostic tool. For non-solid or highly viscous liquids, HR-MAS spectroscopy allows the reduction of most of the line broadening associated with restriction of molecular motion, chemical shift anisotropy, dipolar coupling and field heterogeneity by high-rate spinning of the sample at the magic angle θ=54.7˚ (23,24). The potential of HR-MAS applications to the study of intact tissues (*ex vivo*) has been widely demonstrated and provides further advantages over traditional high resolution liquid NMR of tissue extracts (*in vitro*) (25). High resolution NMR on extracts of excised tissues requires a large amount of a sample (>0.25 g of tissue) (26). Moreover, extraction methods usually discriminate metabolites on the basis of solubility in a particular solvent. Although it has some minor limitations associated mainly to the spinning of the samples (spinning side-bands, degradation effects and temperature gradients among others), HR-MAS is a non-destructive technique, which requires minimal sample preparation, and allows the observation of most of the tissue metabolites and dynamic interactions in an extremely reduced sample quantity. This technology can supplement histopathological examination and improve brain tumour diagnosis (16,27). The similarities between *ex vivo* and *in vivo* spectra found in studies of different primary brain tumours in childhood allow a better interpretation of *in vivo* MR spectra and increase the clinical potential of the method (28,29). HR-MAS spectra generate metabolic profiles that contain information on physiological and pathological status. This approach can be used to define the metabolomic phenotype of a tissue. Previous HR-MAS studies on paediatric brain tumour biopsies showed that correlation between metabolic information obtained *ex vivo* and *in vivo* is quite high (30,31). Additionally, a recent study comparing glial and PNET paediatric brain tumour metabolic profiles by HR-MAS (32) suggested the potential of the technique as a diagnosis support tool for these and other paediatric brain tumours.

The aims of this study are to obtain high resolution NMR metabolic profiles of paediatric ependymomas, medulloblastomas and pilocytic astrocytomas by using ^{1}H HR-MAS, to further characterize these three types of tumours and to identify differences with potential diagnosis value. With that purpose, 20 paediatric brain tumour samples (8 pilocytic astrocytomas, 5 ependymomas and 7 medulloblastomas) underwent ^{1}H HR-MAS spectroscopy measurements. Robust principal component analysis (RPCA) performed over the ^{1}H HR-MAS spectra region between 0.5-4.5 ppm allowed to identify global metabolic patterns of these types of tumours and provided a set of relevant metabolites, which are proposed as potential paediatric brain tumour markers.

Materials and methods

Patient demographics and tissue samples. Twenty tissue samples of paediatric brain tumours were obtained during craniotomy (see tumour localization in Table I) at the Foundation Against the Childhood Neurological Diseases, (FLENI, Argentina). Three types of tumours were included in the study, ependymomas, medulloblastomas and pilocytic astrocytomas. The tissue was collected by an atomopathologist for routine histological analysis. The study was approved by the local ethics committee and informed parental consent was obtained. The remainder tissue was immediately put in cryogenic vials and snap-frozen in liquid nitrogen. All samples used for histopathological examination were fixed in formalin and embedded in paraffin wax by a pathologist. Routine methods

ployed for histopathology studies. All snap-frozen or HR-MAS were stored in at -80˚C until further analysis. Subject ages ranged from 10 months to 15 years.

HR-MAS sample preparation. Total sample preparation time for each sample prior to NMR detection was <5 min. All material to be in contact with the tissue was pre-cooled to reduce tissue degradation during the sample preparation process. Frozen samples were taken from the ultra-freezer and immediately placed in a cryo-vial and in liquid N_2 until insertion in a 4-mm outer diameter ZrO_2 rotor. The HR-MAS tissue sample was split from the whole frozen tumoural mass submerged in liquid nitrogen. The pre-cooled rotor was filled with cooled D_2O after tissue sample insertion. Cylindrical inserts were used in each case, limiting the rotor inner volume to 50 μl. Excess D_2O was removed before rotor sealing. Tissue samples were weighted in the rotor before D_2O addition and HR-MAS measurements. The mean sample weight was 24.2±8.8 mg.

HR-MAS spectroscopy. HR-MAS experiments were conducted in a Bruker Avance DRX 600 spectrometer operating at a ^1H frequency of 600.13 MHz. The instrument was equipped with a 4-mm triple resonance $^1H/^{13}C/^{15}N$ HR-MAS probe with magnetic field gradients aligned with the magic angle axis.

For all experiments, samples were spun at 5,000 Hz to keep the rotation sidebands out of the acquisition window. When possible, consensus protocols developed in multi-center consortiums were used (eTumour). Lock homogeneity was achieved by extensive coil-shimming using the 1D water pre-saturation experiment in interactive mode as control. Alanine doublet at 1.478 ppm was used for lock homogeneity shimming, as described elsewhere (19). Nominal temperature of the sample receptacle was kept at 273 K, using the cooling of the inlet gas pressures responsible for the sample spinning. This value corresponded to the temperature measured from the thermocouple just below the rotor in the probe. The effect of sample rotation was to slightly increase this value. Internal measurement using a 100% MeOH sample in a 4-mm rotor spinning at the same frequency provided a corrected internal value of 277 K. In order to minimize the effects of tissue degradation, which would alter the metabolite composition of the biopsy, all *ex vivo* spectra were acquired at this temperature of 277 K. A total of 10 min was allowed for the temperature of the sample to reach a steady state before spectra were acquired. A single-pulse pre-saturation experiment was acquired in all samples. Number of transients was 256 collected into 32 k data points for all experiments. Water pre-saturation was used for 1 sec during recycling delay for solvent signal suppression. Spectral widths were 8,000 Hz for ^1H. Before Fourier transformation, the free induction decay was zero filled and multiplied with a 0.3 Hz exponential line broadening. Chemical shift referencing was performed relative to the Alanine CH_3 signal at 1.478 ppm. For assignment purposes, two-dimensional (2D) homo- (2D-TOCSY) and heteronuclear (2D-1H,13C-HSQC) experiments were acquired from selected samples.

Spectral analysis. All 20 spectra were processed using TopSpin 1.5 (Bruker Biopsin GmbH, Rheinstetten, Germany) and transferred to MatLab (MathWorks Inc, 2006) using in-house scripts for data analysis. The chemical shift region including resonances between 0.50-4.50 ppm (the aliphatic region) was investigated. The spectra were normalized to total aliphatic spectral area to eliminate differences in sample weight. The spectra were binned into 0.01 ppm buckets and statistical analysis was performed using in-house MatLab scripts and the Libra statistical multivariate analysis library (33). RPCA was applied to the set of spectral vectors. Principal components were chosen to explain at least 80% of the variance. The loading plots of the corresponding Principal Components were used to detect most discriminative metabolites. Signals belonging to these selected metabolites were integrated and quantified. One-way analysis of variance (ANOVA) was used for the determination of statistical significance of the corresponding integrals among medulloblastomas, pilocytic astrocytomas and ependymomas by group means. The significance of the test was determined at $p<0.05$.

Results and Discussion

Primary brain tumours are proportionately less frequent than other cancers, but they are the second highest cause of death from cancer in children, after leukaemia. Paediatric brain tumours are distinct from those in adults, and many different tumour types are encountered in clinical practice. Childhood glial and neuroglial tumours are complex disease processes that have various patterns of histological features, with subsets of tumours that differ markedly in the expected survival time. Additionally, although most childhood glial and neuroglial tumours are of low grade and respond to therapy, their diagnosis, and hence the selection of the appropriate treatment, are often complicated because of their location, which is usually adjacent to crucial structures and thus restricts the options for diagnostic biopsies. There is a great need for increasing our understanding of brain tumour biology to improve diagnosis, prognosis and develop, guide and monitor treatments. Metabolic profiling of biopsies opens new possibilities for better characterization of tumour biology and better classification of tumour samples. The PCA analysis of spectra obtained in this study showed differential metabolic patterns among different paediatric brain tumours. Our results show that high resolution NMR spectroscopy may be a useful tool for supporting and refining histopathology in the diagnosis of paediatric brain tumours.

Spectral features. All NMR spectra recorded showed narrow line widths and high signal-to-noise ratios with well-resolved spin-spin multiplicities. Representative ^1H HR-MAS spectra of paediatric medulloblastoma, ependymoma and pilocytic astrocytoma are shown in Fig. 1. HR-MAS spectra exhibit a higher signal-to-noise ratio and resolution than *in vivo* spectra, allowing the identification and quantification of many more resonances (Fig. 2). Metabolite spin systems and resonances were identified by using literature data (30,31) and additional 2D homo and multi-nuclear experiments collected in selected samples. The 1D single-pulse pre-saturation experiment provides complete and unambiguous identification of the metabolic pattern characterizing the examined tissues. Resonances from most relevant metabolites are shown in Figs. 1 and 2. In all spectra, the aliphatic region had prominent

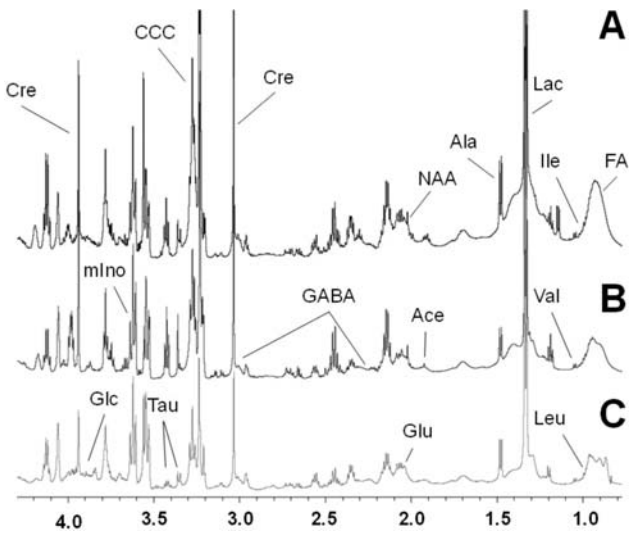

Figure 1. Comparison of typical ^{1}H HR-MAS spectra for intact tissue from paediatric pilocytic astrocytoma (A), medulloblastoma (B) and ependymoma (C). Most relevant resonances have been labeled. FA, fatty acids; Ile, isoleucine; Lac, lactate; Val, valine; Leu, leucine; Ala, alanine; Glu, glutamate; Ace, acetate; NAA, N-acetyl-aspartate; GABA, γ-aminobutyric acid; Cre, creatine; CCC, choline-containing compounds; Tau, taurine; mIno, myo-inositol; Glc, glucose.

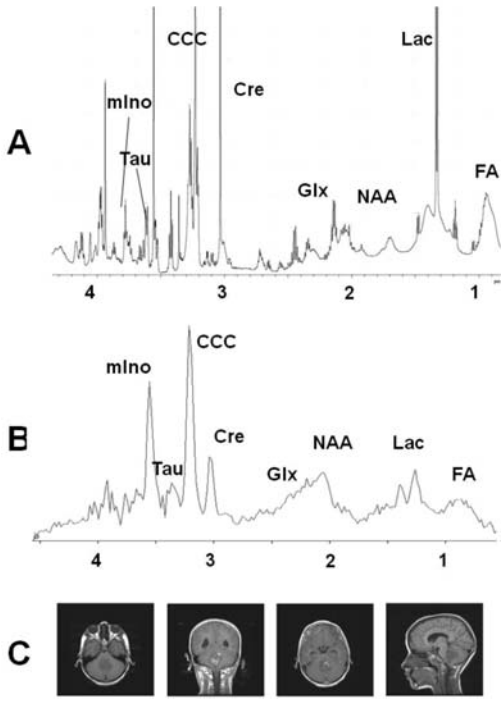

Figure 2. Comparative example of improved resolution in ^{1}H HR-MAS spectrum (A), with respect to MRS *in vivo* spectrum (B) for a paediatric medulloblastoma. MRI images (C) show the location of the tumour.

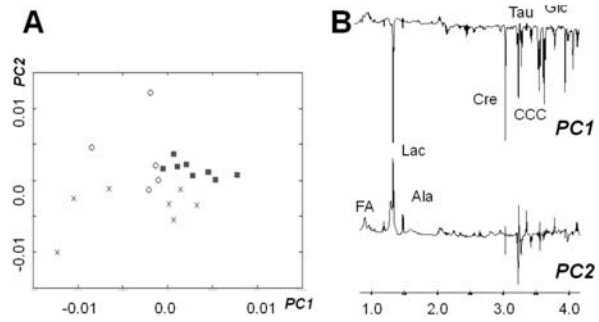

Figure 3. Scores (A) and loadings (B) plots for principal component analysis (RPCA) to compare the metabonome of paedriatic medulloblastomas (x), ependymomas (white circles) and pilocytic astrocytoma (black squares) based on ^{1}H HR-MAS 1D presaturation single-pulse experiment.

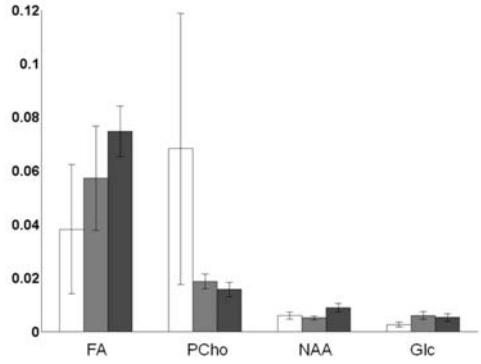

Figure 4. Histogram showing metabolite levels for medulloblastoma (white), ependymoma (light grey) and pilocytic astrocytoma (dark gray) paediatric brain tumours with statistical significance ($p<0.01$) and relevance to tumour metabolism.

signals of water-soluble metabolites such as lactate, creatine, taurine, phosphoethanolamine (PEA), glycerophosphocholine (GPCho), phosphocholine (PCho), and choline (Cho). Choline-containing compounds, which are highly overlapped in *in vivo* spectra, were resolved by *ex vivo* ^{1}H HR-MAS spectroscopy detecting separately the three different peaks of GPCho, PCho and free-Cho, free-Cho and PCho being the most prominent signals found in all groups of tumours. This suggests that they are the main contribution to the total signal detected and reported in the *in vivo* MRS studies at low-field strength (1.5-3.0 T). This distinction is important because PCho appears to play a role in carcinogenesis through the overexpression of choline kinase (34). Multiplets hardly resolved in conventional clinical scanners (1.5-3.0 T), such as glutamine and glutamate, were clearly identified by HR-MAS spectroscopy. The endogenous compounds detected in the spectra also include standard amino acids such as glycine, leucine, isoleucine, valine, alanine, lysine, asparagine and aspartic acid. Other signals observed included glucose and γ-aminobutyric acid (GABA). Prominent broad signals belonging to lipids and fatty acid chains were also detected.

The risk of overestimating statistical significance in the study of small data sets may be partially overcome by performing RPCA of the data. RPCA reduces the complexity of the data in a rational way without prior knowledge, generating an unbiased overview of the data, allowing observation of metabolical sample similarities in the scores plot. RPCA was carried out on the mean-centered normalized ^{1}H NMR spectra to generate an overview of the variations among groups. Two principal components were calculated for the model with a total of 90% of variance being expressed. While complete discrimination was not achieved, our RPCA results exhibit some interesting trends in the differentiation of the types of

Relative intensity area, frequency position and p-values for statistically significant ($p<0.01$) metabolites.

Metabolite	δ ppm	Medulloblastoma	Ependymoma	Pilocytic astrocytoma	P-value
Fatty acids	0.80	0.038±0.024	0.057±0.019	0.075±0.010	0.0046
Leucine	0.96	0.006±0.001	0.007±0.002	0.009±0.002	0.0088
Isoleucine	1.00	0.004±0.001	0.005±0.002	0.007±0.001	0.0069
Valine	1.04	0.002±0.001	0.002±0.001	0.003±0.0004	0.0009
PCho	3.22	0.068±0.050	0.019±0.003	0.016±0.003	0.0074
GABA	1.89	0.001±0.001	0.001±0.001	0.002±0.0003	0.0063
Acetate	1.90	0.002±0.001	0.001±0.001	0.003±0.001	0.0032
NAA	2.02	0.006±0.001	0.005±0.001	0.009±0.002	0.0002
Glutamate	2.04	0.007±0.001	0.008±0.002	0.011±0.003	0.0011
Glutamine	2.42	0.012 ±0.003	0.011±0.003	0.015±0.002	0.0155
GPCho/PCho	3.23	0.020±0.009	0.018±0.004	0.010±0.004	0.0074
Glycine	3.62	0.005±0.002	0.006±0.002	0.003±0.001	0.0046
Myo-inositol	3.61	0.012±0.008	0.009±0.004	0.004±0.001	0.0036
Glucose	3.90	0.003±0.001	0.006±0.002	0.005±0.001	0.0003
Creatine	3.93	0.003±0.001	0.006±0.001	0.005±0.001	0.0006
Serine	3.98	0.012±0.004	0.006±0.001	0.001±0.001	0.0002
Phenylalanine	4.00	0.002±0.001	0.003±0.001	0.002±0.001	0.0059
Taurine	3.42	0.008±0.007	0.002±0.002	0.001±0.001	0.0077

tumours studied here, as shown in Fig. 3A. Pilocytic astrocytomas form a well-defined group. Interestingly, the different principal components PC1 and PC2 seem to help in the discrimination of different pairs of tumours. PC1 provides a good basis for the metabolic differentiation between ependymomas and pilocytic astrocytomas, whereas PC2 provides the basis for distinguishing between medulloblastomas and the other groups. Fig. 3B shows the corresponding RPCA loading plots (PC1 and PC2). Spectral integration was performed over the most significant signals. Statistically significant intensity values, according to the ANOVA test, are summarized in Table II. Relative levels of metabolites relevant for tumour metabolism have been plotted in Fig. 4.

Metabolic profile of medulloblastoma. Medulloblastoma ^{1}H HR-MAS spectra were characterized by high levels of taurine, GPCho, PCho and free-Cho. An example of ^{1}H HR-MAS spectra in this type of tumour is presented in Figs. 1 and 2. Recent studies have shown that taurine can affect nerve blood flow, motor nerve conduction velocity, and nerve sensory thresholds (35). An increase in taurine has been correlated with malignancy (36), possibly related to an increased blood perfusion in the aggressive tumour. The increase in choline-containing compounds also suggests a very active tumour. Increased levels of PCho have been related to the Ras oncogene activation (37) and to higher total choline-containing compound levels. Choline-containing compounds, which are involved in membrane synthesis and degradation, are associated with increased membrane turnover and tumour growth (38). In contrast, levels of NAA, which are typically associated with neuronal viability, and creatine, related to energy metabolism, are decreased in medulloblastomas, suggesting neuronal death. Myo-inositol also exhibits a slight increase in medulloblastoma with respect to other paediatric brain tumours. Interestingly, medulloblastomas, which are the most aggressive tumours examined in this study, show the lowest levels of total fatty acids. The interpretation of variations in these signals is far from simple. Mobile lipids are typically associated with malignancy in a variety of paediatric brain tumours (39). However, they are also correlated with other cell processes such as apoptosis, metabolic cell stress and loss of viability (40). Glucose levels in medulloblastoma are also rather low. In previous studies it was hypothesized that malignant tumours have a high metabolic rate (41). Additionally, some reports showed correlation between glucose consumption rate and lactate levels for gliomas, suggesting alterations in glycolysis in brain tumours (42). However, we did not find a statistically significant correlation between lactate levels and tumour grade. There is an unavoidable warm ischaemia period in sampling the brain tumour sections prior to snap freezing. As a consequence, anaerobic glycolysis is activated and glucose and lactate levels determined in these samples may be affected. This possibly hampers the detection of statistical correlations in these metabolites. Our findings support the previous *ex vivo* and *in vivo* results reported at short echo times regarding levels of taurine as the most discriminant metabolite of medulloblastoma (11,32). Overall, the HR-MAS profile of paediatric medulloblastomas provides important metabolic information including an increased membrane turnover, low neuronal viability and glycolysis alterations.

Metabolic profile of pilocytic astrocytoma. Pilocytic astrocytomas, WHO grade I brain tumours, show higher concentration of fatty acids, as can be seen in Fig. 1. This suggests that fatty acids are not exclusively related to necrosis and apoptosis. Increased fatty acid levels may also represent an alteration in the metabolism of mobile lipids in this particular pathology. Fatty acid metabolism may also contribute to energy production in the developing brain.

Other characteristic features of HR-MAS spectra of paediatric pilocytic astrocytoma include low levels of creatine, myo-inositol and taurine, in agreement with previous studies (32). Additionally, we found that all choline-containing compounds were in low concentrations in these brain tumours, reflecting their low aggressiveness. Amino acids such as isoleucine, leucine and valine were detected in higher concentrations in pilocytic astrocytoma when compared to other tumours. NAA, as expected, is present at higher levels in this group in comparison with other types of tumours, suggesting low levels of neuronal destruction. Additionally, and supporting this observation, neurotransmitter and neuroinhibitors are present at higher levels in these tumours. GABA and especially glutamate show higher concentrations in comparison with the other tumours studied here. Pilocytic astrocytomas display a typical metabolic profile of low grade glial tumours, where neuronal viability is still high and the tumour growth, represented by choline-containing compounds, remains moderate.

Metabolic profile of ependymoma. To the best of our knowledge, this is the first metabolic profiling study of paediatric brain tumours including as many as five paediatric ependymoma biopsies. Paediatric ependymoma HR-MAS spectra are mainly characterized by intense signals of myo-inositol. Myo-inositol is normally elevated in the newborn brain, but its concentration rapidly decreases thereafter. Myo-inositol is also involved in the activation of protein kinase C. This protein leads to production of proteolytic enzymes, which are found more often in malignant and aggressive primary cerebral tumours. Thus, changes in the levels of myo-inositol may predict the histological grade of brain tumours (43). Interestingly, levels of NAA in ependymoma are very similar to those in medulloblastoma. However, the average age of the ependymoma group is also slightly lower, and therefore, a decreased NAA level is also expected in the healthy developing brain. Other metabolic features observed in paediatric ependymomas include slightly lower levels of GABA, PCho, and GPCho with respect to medulloblastoma. The levels of choline-containing compounds in ependymoma with respect to medulloblastoma are in good agreement with lower tumour grade. GABA is the principal inhibitory neurotransmitter in the adult mammalian brain and is thought to also be involved in cell proliferation, migration and promotion of cell survival. Given that GABA participates in the proliferation of various normal cell types, a role in cancer cell proliferation has been considered. Increased GABA content has been reported in several types of cancers, colon, breast, prostate gastric and glioma (44,45). Previous studies using purified brain tumour cell cultures (or primary cultures of neural cells) have shown that most of the tumour cells do not express NAA or GABA, but rather only tumour cells derived from neurons do. Florian *et al* (46) reported that while neuroblastoma cells have a significant concentration of GABA and NAA, glioblastoma cells show <10% of GABA and no NAA at all. Similarly, other studies showed that astrocytes and oligodendrocytes contain <10% of GABA levels seen in neurons (47). The presence of either compounds in astrocytomas and ependymomas are likely to reflect contributions by neuronal cells in the samples. Another interesting feature of paediatric ependymoma spectra is the high levels of phenylalanine. Although the role of phenylalanine in cancer is unclear, it can be neurotoxic and it can affect the synthesis of inhibitory monoamine neurotransmitters (48). In general, levels of other important metabolites in the characterization of brain tumours, such as fatty or amino acids, suggest an intermediate metabolic situation between medulloblastomas and pilocytic astrocytomas. Overall, the metabolic profile of paediatric ependymomas confirms that these tumours are less aggressive than medulloblastoma but more than grade I pilocytic astrocytoma.

In summary, the metabolic characterization of paediatric brain tumour tissue by HR-MAS NMR spectroscopy provided differential patterns for ependymoma, medulloblastoma, and pilocytic astrocytoma. The metabolic composition of the tumour tissue was highly consistent in previous *in vivo* and *ex vivo* studies. We report here, for the first time, a metabolic profile of several paediatric ependymoma biopsies. This metabolic profile confirms that ependymoma is a tumour with a biochemical aggressiveness inbetween the aggressiveness of medulloblastoma and pilocytic astrocytoma. Agreement between *in vivo* and *ex vivo* MR spectroscopy suggests that *ex vivo* HR-MAS spectroscopy can improve spectral resolution and provide a link between *in vivo* spectroscopy and neuropathological analysis of paediatric brain tumours. Particular attention should be placed on choline-containing compounds and glutamate metabolites, which are hardly resolved in common clinical scanners. Despite the limited number of cases per type of tumour, a trend was observed for the separation of them using RPCA and the ANOVA test. Some resonances detected in this work and not previously obtained by *in vivo* spectroscopy showed some potential as aids for tumour typing and grading. The corresponding metabolites include GABA, glucose, and some amino acids. However, their metabolic role in the disease is not well understood yet. Other metabolites, typically observed in adult brain tumours, correlate well with tumour grade. Interestingly, mobile lipids, which have not been previously studied by *ex vivo* HR-MAS in paediatric tumours, decrease with tumour grade. Overall, this work suggests that the additional information obtained by *ex vivo* HR-MAS metabolic profiling of paediatric brain tumours may be useful for assessing tumour grade and support histopathology analysis.

Acknowledgements

SAF 2008-00270 project from the Ministry of Science and Innovation of Spain, ACOMP/2009/200 project from the Consellería de Educación of the Generalitat Valenciana and AP076/08 project from the Consellería de Sanidad of the Generalitat Valenciana, to D.M., are gratefully acknowledged for their financial support. D.M. also gratefully acknowledges a Ramon y Cajal contract from the Ministry of Education of Spain. SAF2007-65473 project from the Ministry of Science and Innovation of Spain and eTumour project (FP6-2002-LIFESCIHEALTH 503094) from the FP6 European Comission to B.C. are also gratefully acknowledged. SC gratefully acknowledges a fellowship from Banco Santander-BANESPA.

References

1. Louis DN, Ohgaki H, Wiestler OD, Cavenee WK, Burger PC, Jouvet A, Scheithauer BW and Kleihues P: The 2007 WHO Classification of tumors of the central nervous system. Acta Neuropathol 114: 97-109, 2007.

blum MK and Bigner DD: Pathology of tumors of the nervous system. 7th ed. Oxford University Press, New York 2006.
3. Larouche V, Huang A, Bartels U and Bouffet E: Tumors of the central nervous system in the first year of life. Pediatr Blood Cancer 49: 1074-1082, 2007.
4. Saran F: Recent advances in paediatric neuro-oncology. Curr Opin Neurol 15: 671-677, 2002.
5. Brandes AA and Paris MK: Review of the prognostic factors in medulloblastoma of children and adults. Crit Rev Oncol Hematol 50: 121-128, 2004.
6. Panigrahy A, Krieger MD, Gonzalez I, Liu X, McComb JG, Finlay JL, Nelson MD, Gilles FH and Blüml S: Quantitative short echo time ^{1}H-MR spectroscopy of untreated pediatric brain tumors: preoperative diagnosis and characterization. Am J Neuroradiol 27: 560-572, 2006.
7. Hwang JH, Egnaczyk GF, Ballard E, Scott R, Holland SK and Ball WS: Proton MR Spectroscopic Characteristics of pediatric pilocytic astrocytomas. Am J Neuroradiol 19: 535-540, 1998.
8. Wang Z, Zimmerman RA and Sauter R: Proton MR Spectroscopy of the brain: clinically useful information obtained in assessing CNS disease in children. AJR 167: 191-194, 1996.
9. Marcus KJ, Astrakas LG, Zurakowski D, Zarifi MK, Mintzopoulos D, Young T, Anthony DC, Girolami U, Black P, Tarbell NJ and Tzika AA: Predicting survival of children with CNS tumors using proton magnetic resonance spectroscopic imaging biomarkers. Int J Oncol 30: 651-657, 2007.
10. Hourani R, Horská A, Albayram S, Brant LJ, Melhem E, Cohen KJ, Burger PC, Weingart JD, Carson B, Wharam MD and Barker PB: Proton Magnetic Resonance Spectroscopic Imaging to differentiate between nonneoplastic lesions and brain tumors in children. J Mag Res Imag 23: 99-107, 2006.
11. Astrakas LG, Zurakowski D, Tzika AA, Zarifi MK, Anthony DC, De Cgirolami U, Tarbell NJ and McLaren P: Noninvasive magnetic resonance spectroscopic imaging biomarkers to predict the clinical grade of pediatric brain tumors. Clinic Cancer Res 10: 8220-8228, 2004.
12. Teo C, Nakaji P, Symons P, Tobias V, Cohn R and Smee R: Ependymoma. Childs Nerv Syst 19: 270-285, 2003.
13. Kayama T, Tominaga T and Yoshimoto T: Management of pilocytic astrocytoma. Neurosurg Rev 19: 217-220, 1996.
14. Harris LM, Davies NP, Macpherson L, Lateef S, Natarajan K, Brundler MA, Sgouros S, English MW, Arvanitis TN, Grundy RG and Peet AC: Magnetic resonance spectroscopy in the assessment of pilocytic astrocytomas. Eur J Cancer 44: 2640-2647, 2008.
15. Peet AC, Lateef S, MacPherson L, Natarajan K, Sgouros S and Grundy RG: Short echo time 1H magnetic resonance spectroscopy of childhood brain tumours. Childs Nerv Syst 23: 163-169, 2007.
16. Cheng LL, Ma MJ, Becerra L, Ptak T, Tracey I, Lackner A and González RG: Quantitative neuropathology by high resolution magic angle spinning proton magnetic resonance spectroscopy. Proc Natl Acad Sci USA 94: 6408-6413, 1997.
17. Payne GS, Troy H, Vaidya SJ, Griffiths JR, Leach MO and Chung YL: Evaluation of ^{31}P high-resolution magic angle spinning of intact tissue samples. NMR Biomed 19: 593-598, 2006.
18. Chen JH, Sambol EB, Kennealey PT, O'Connor RB, DeCarolis PL, Cory DG and Singer S: Water suppression without signal loss in HR-MAS 1H NMR of cells and tissues. J Magn Reson 171: 143-150, 2004.
19. Griffin JL, Bollard M, Nicholson JK and Bhakoo K: Spectral profiles of cultured neuronal and glial cells derived form HR MAS (1)H NMR spectroscopy. NMR Biomed 15: 375-384, 2002.
20. Bathen TF, Jensen LR, Sitter B, Fjösne HE, Halgunset J, Axelson DE, Gribbestad IS and Lundgren S: MR-determined metabolic phenotype of breast cancer in prediction of lymphatic spread, grade, and hormone status. Breast Cancer Res Treat 104: 181-189, 2007.
21. Swanson MG, Zektzer AS, Tabatabai ZL, Simko J, Jarso S, Keshari KR, Schmitt L, Carroll PR, Shinohara K, Vigneron DB and Kurhanewicz J: Quantitative analysis of prostate metabolites using 1H HR-MAS spectroscopy. Magn Reson Med 55: 1257-1264, 2006.
22. Monleón D, Morales JM, Gonzalez-Darder J, Talamantes F, Cortés O, Gil-Benso R, López-Ginés C, Cerdá-Nicolás M and Celda B: Benign and atypical meningioma metabolic signatures by high-resolution magic-angle spinning molecular profiling. J Proteome Res 7: 2882-2888, 2008.
23. Andrew ER and Eades RG: Removal of dipolar broadening of NMR spectra of solids by specimen rotation. Nature 183: 1802, 1959.
24. Garroway AN: Magic angle sample spinning of liquids. J Magn Reson 49: 168-171, 1982.
25. Waters NJ, Holmes E, Waterfield CJ, Farrant RD and Nicholson JK: NMR and pattern recognition studies on liver extracts and intact livers from rats treated with alpha-naphthylisothiocyanate. Biochem Pharmacol 64: 67-77, 2002.
26. Maxwell RJ, Martinez-Perez I, Cerdan S, Cabanas ME, Arus C, Moreno A, Capdevila A, Ferrer E, Bartomeus F, Aparicio A, Conesa G, Roda JM, Carceller F, Pascual JM, Howells SL, Mazucco R and Griffiths JR: Pattern recognition analysis of 1H NMR spectra from perchloric acid extracts of human brain tumor biopsias. Magn Reson Med 39: 869-877, 1998.
27. Cheng LL, Chang IW, Louis DN and Gonzalez RG: Correlation of high-resolution magic angle spinning proton magnetic resonance spectroscopy with histopathology of intact human brain tumor specimens. Cancer Res 58: 1825-1832, 1998.
28. Sutton LN, Wehrli SL, Gennarelli L, Wang Z, Zimmerman R, Bonner K and Rorke LB: High-resolution ^{1}H-magnetic resonance spectroscopy of pediatric posterior fossa tumors in vitro. J Neurosurg 81: 443-448, 1994.
29. Tzika AA, Cheng LL, Goumnerova L, Madsen JR, Zurakowski D, Astrakas LG, Zarifi MK, Scott RM, Anthony DC, Gonzalez RG and Black P: Biochemical characterization of pediatric brain tumors by using in in vivo and ex vivo magnetic resonance spectroscopy. J Neursosurg. 96: 1023-1031, 2002.
30. Tugnoli V, Schenetti L, Mucci A, Nocetti L, Toraci C, Mavilla L, Basso G, Rovati R, Tavani F, Zunarelli E, Righi V and Tosi MR: A comparison between *in vivo* and *ex vivo* HR-MAS ^{1}H MR spectra of a pediatric posterior fossa lesion. Int J Mol Med 16: 301-307, 2005.
31. Wilson M, Davies NP, Grundy RG and Peet AC: A quantitative comparison of metabolite signals as detected by in vivo MRS with ex vivo 1H HR-MAS for childhood brain tumours. NMR Biomed 22: 213-219, 2009.
32. Wilson M, Davies NP, Brundler MA, McConville C, Grundy RG and Peet AC: High resolution magic angle spinning 1H NMR of childhood brain and nervous system tumours. Mol Cancer 8: 6, 2009.
33. Verboven S and Hubert M: LIBRA: a MATLAB library for robust analysis. Chemometrics Intelligent Lab Systems 75: 127-136, 2005.
34. Ramírez de Molina A, Rodríguez-González A, Gutiérrez R, Martínez-Piñeiro L, Sánchez J, Bonilla F, Rosell R and Lacal J: Overexpression of choline kinase is a frequent feature in human tumor-derived cell lines and in lung, prostate, and colorectal human cancers. Biochem Biophys Res Commun 296: 580-583, 2002.
35. Li F, Abatan OI, Kim H, Burnett D, Larkin D, Obrosova IG and Stevens MJ: Taurine reverses neurological and neurovascular deficits in Zucker diabetic fatty rats. Neurobiol Dis 22: 669-676, 2006.
36. Kim C: Accumulation of taurine in tumor and inflammatory lesions. Adv Exp Med Biol 583: 213-217, 2006.
37. Ronen SM, Jackson LE, Beloueche M and Leach MO: Magnetic resonance detects changes in phosphocholine associated with Ras activation and inhibition in NIH 3T3 cells. Br J Cancer 84: 691-696, 2001.
38. Wang Z, Sutton LN, Cnaan A, Haselgrove JC, Rorke LB, Zhao H, Bilaniuk LT and Zimmerman RA: Proton MR Spectroscopy of pediatric cerebellar tumors. Am J Neuroradiol 16: 1821-1833, 1995.
39. Kuesel AC, Donnelly SM, Halliday W, Sutherland GR and Smith IC: Mobile lipids and metabolic heterogeneity of brain tumours as detectable by ex vivo 1H MR spectroscopy. NMR Biomed 7: 172-180, 1994.
40. Blankenberg FG, Katsikis PD, Storrs RW, Beaulieu C, Spielman D, Chen JY, Naumovski L and Tait JF: Quantitative analysis of apoptotic cell death using proton nuclear magnetic resonance spectroscopy. Blood 89: 3778-3786, 1997.
41. Di Chiro G, DeLaPaz RL, Brooks RA, Sokoloff L, Kornblith PL, Smith BH, Patronas NJ, Kufta CV, Kessler RM, Johnston GS, Manning RG and Wolf AP: Glucose utilization of cerebral gliomas measured by [18F] flurodeoxyglucose and positron emission tomography. Neurology 32: 1323-1329, 1982.
42. Luyten PR, Marien AJH, Heindel W, van Gerwen PH, Herholz K, den Hollander JA, Friedmann G and Heiss WD: Metabolic imaging of patients with intracranial tumors: H-1 MR spectroscopic imaging and PET. Radiology 176: 791-799, 1990.

43. Castillo M, Smith JK and Kwock L: Correlation of myo-inositol levels and grading of cerebral astrocytomas. Am J Neuroradiol 21: 1645-1649, 2000.
44. Watanabe M, Maemura K, Oki K, Shiraishi N, Shibayama Y and Katsu K: Gamma-aminobutyric acid (GABA) and cell proliferation: focus on cancer cells. Histol Histopathol 21: 1135-1141, 2006.
45. Azuma H, Inamoto T, Sakamoto T, Kiyama S, Ubai T, Shinohara Y, Maemura K, Tsuji M, Segawa N, Masuda H, Takahara K, Datsuoka Y and Watanabe M: Gamma-aminobutiric acid as a promoting factor of cancer metastasis; induction of matrix metalloproteinase production is potentially its underlying mechanism. Cancer Res 63: 8090-8096, 2003.
46. Girard N, Wang ZJ, Erbetta A, Sutton LN, Phillips PC, Rorke LB and Zimmerman RA: Prognostic value of proton MR spectroscopy of cerebral hemisphere tumours in children. Neuroradiology 40: 121-125, 1998.
47. Florian CL, Preece NE, Bhakoo KK, Williams SR and Noble M: Characteristic metabolic profiles revealed by 1H NMR spectroscopy for three types of human brain and nervous system tumours. NMR Biomed 8: 253-264, 1995.
48. Urenjak J, Williams SR, Gadian DG and Noble M: Proton nuclear magnetic resonance spectroscopy unambiguously identifies different neural cell types. J Neurosci 13: 981-989, 1993.